CrossMark

ORIGINAL ARTICLE

Long-term prediction of polar motion using a combined SSA and ARMA model

Yi Shen[1] · Jinyun Guo[1,2] · Xin Liu[1] · Qiaoli Kong[1,2] · Linxi Guo[1] · Wang Li[3]

Abstract To meet the need for real-time and high-accuracy predictions of polar motion (PM), the singular spectrum analysis (SSA) and the autoregressive moving average (ARMA) model are combined for short- and long-term PM prediction. According to the SSA results for PM and the SSA prediction algorithm, the principal components of PM were predicted by SSA, and the remaining components were predicted by the ARMA model. In applying this proposed method, multiple sets of PM predictions were made with lead times of two years, based on an IERS 08 C04 series. The observations and predictions of the principal components correlated well, and the SSA + ARMA model effectively predicted the PM. For 360-day lead time predictions, the root-mean-square errors (RMSEs) of PMx and PMy were 20.67 and 20.42 mas, respectively, which were less than the 24.46 and 24.78 mas predicted by IERS Bulletin A. The RMSEs of PMx and PMy in the 720-day lead time predictions were 28.61 and 27.95 mas, respectively.

Keywords Polar motion prediction · Singular spectrum analysis · Autoregressive moving average · Root-mean-square error

✉ Jinyun Guo
  jinyunguo1@126.com

1 College of Geodesy and Geomatics, Shandong University of Science and Technology, Qingdao 266590, China

2 State Key Laboratory of Mining Disaster Prevention and Control Cofounded by Shandong Province and Ministry of Science and Technology, Shandong University of Science and Technology, Qingdao 266590, China

3 School of Earth Science and Engineering, Hohai University, Nanjing 211100, China

1 Introduction

The polar motion (PM) of the Earth is the rotation axis movement with respect to its crust. PMs can be accurately determined with space geodetic techniques. However, due to the complexity of data acquisition and processing, the results cannot be provided in real time (Bizouard and Gambis 2009; Schuh and Behrend 2012). The high accuracy of the PM parameters is necessary to determine the relationship between the terrestrial reference frame and the celestial reference frame. This is important for researches and applications such as satellite navigation and positioning and spacecraft tracking (Kalarus et al. 2010; Xu et al. 2012; Choi et al. 2013). The reliable and accurate prediction of PM has the important scientific and practical value.

Long-term observations indicate that PMs have the Chandler oscillation, and seasonal, sub-seasonal, interannual, and long-term changes. The Chandler and annual oscillations are the most important of these changes (Schuh et al. 2001; Guo and Han 2009; Shen et al. 2015). Commonly, extrapolative prediction models are constructed based on the deterministic periods of PM using the least squares (LS) harmonic fitting trend term and periodic terms, and then to use a deterministic or stochastic model to predict its residual (Kosek et al. 1998; Akulenko et al. 2002; Yao et al. 2013). Among these existing models, the LS + AR model is currently considered to be one of the most effective for short- and long-term forecasting of PM (Kosek et al. 2007; Kalarus et al. 2010; Xu and Zhou 2015). Due to the complexity of the physical excitation mechanism and time variations of the main periodic oscillations of PM (Chen and Wilson 2005), the fitting of the data series using the LS fitting model of the trigonometric function does not accurately reflect the period and trend terms variations. This inaccuracy has a significant influence on the accuracy of long-term PM predictions. PM has very

complex nonlinear characteristics because it is affected by a variety of excitation sources (Jin et al. 2012). Many groups have used nonlinear models to predict PM, such as an adaptive neural network fuzzy inference system (Akyilmaz and Kutterer 2004; Akyilmaz et al. 2011) and an artificial neural network (Schuh et al. 2002; Liao et al. 2012). These previous studies have shown that neural networks and other nonlinear models can play a significant role in PM prediction. Su et al. (2014) used a normal time–frequency transform to analyze the time and frequency domains of PM and to construct a PM prediction model, which has achieved good results in single- and multi-year forecasts.

The singular spectrum analysis (SSA) (Broomhead and King 1986), a nonparametric spectral estimation method, combines elements of classical time series analysis, multivariate statistics, multivariate geometry, dynamical systems, and signal processing. This analytical method can effectively identify and display the periodic signal of a time series, allowing the precise separation and reconstruction of its principal components. SSA has been used in oceanography (Kondrashov and Berloff 2015), climatology (Wyatt et al. 2012; Rial et al. 2013), surveying (Chen et al. 2013; Wang et al. 2016), and in other fields that involve component analyses of time series. The SSA method can extract accurate principal component information from an incomplete sequence and then determine a suitable data interpolation model (Schoellhamer 2001; Beckers and Rixen 2003). As shown by the temporal or spatial correlation of the data, SSA can decompose and reconstruct the main components of a data set, which can then be used to approximate the missing data. Kondrashov and Ghil (2006) and Kondrashov et al. (2010) proposed the repeated iterative reconstruction of the principal components by SSA in the interpolation of incomplete solar wind data and determined the window size, M, and the number of reconstructed components (RCs), k, for SSA by cross validation.

This paper is organized as follows: The principles of SSA and the SSA of PM are discussed in Sect. 2. The SSA and ARMA method used for PM prediction are presented in Sect. 3. In Sect. 4, we discuss the results of applying the prediction method to PM over multiple periods. Our conclusions are given in Sect. 5.

2 Singular spectrum analysis of polar motion

SSA is a statistical technique which is related to the empirical orthogonal function (EOF) determined from the dynamic reconstruction of a sequence. SSA is practically a special application of EOF decomposition. In SSA, a trajectory matrix is constructed for a one-dimensional nonlinear time series. This matrix can be decomposed and reconstructed to extract various components of the original time series, such as the long-term trend, the periodic terms, or noise (Vautard and Ghil 1989.

2.1 Principle of SSA

A daily time series $\{x_N\}$ has a length N. The trajectory matrix X is constructed by selecting the appropriate window size M ($M < N/2$) for the one-dimensional time series. The trajectory matrix X can be given as

$$X = \begin{bmatrix} x_1 & x_2 & \cdots & x_{N-M+1} \\ x_2 & x_3 & \cdots & x_{N-M+2} \\ \vdots & \vdots & \ddots & \vdots \\ x_M & x_{M+1} & \cdots & x_N \end{bmatrix}. \tag{1}$$

Then, the autocovariance matrix Tx (the Toeplitz matrix) of the trajectory matrix X is obtained by

$$T_X = \begin{bmatrix} c(0) & c(1) & \cdots & c(M-1) \\ c(1) & c(0) & \cdots & c(M-2) \\ \vdots & \vdots & \ddots & \vdots \\ c(M-1) & c(M-2) & \cdots & c(0) \end{bmatrix}, \tag{2}$$

where $c(j) = \frac{1}{N-j}\sum_{i=1}^{N-j} x_i x_{i+j}$, $j = 0, 1, \ldots, M-1$. $c(j)$ is the unbiased autocovariance function. The eigenvalues, $\lambda_1 \geq \lambda_2 \geq \cdots \geq \lambda_M$, and eigenvectors of T_X can then be determined. The eigenvector $E_{j,k}$, corresponding to λ_k is the temporal empirical orthogonal function (T-EOF). Projecting the time series onto $E_{j,k}$ gives the corresponding temporal principal component (T-PC)

$$a_{i,k} = \sum_{j=1}^{M} x_{i+j} E_{j,k}, \tag{3}$$

where $0 \leq i \leq N - M$, $1 \leq j \leq M$. SSA separates the components, so the reconstructed component (RC) can be determined from the resulting T-EOF and T-PC. The kth RC is

$$x_{i,k} = \begin{cases} \frac{1}{i}\sum_{j=1}^{i} a_{i-j+1,k} E_{j,k}, & 1 \leq i \leq M-1 \\ \frac{1}{M}\sum_{j=1}^{i} a_{i-j+1,k} E_{j,k}, & M \leq i \leq N-M+1 \\ \frac{1}{N-i+1}\sum_{j=i-N+M}^{M} a_{i-j+1,k} E_{j,k}, & N-M+2 \leq i \leq N. \end{cases} \tag{4}$$

SSA can reconstruct M components in which the RCs of a low-frequency signal effectively express the main variation characteristics of the original series, and the series can be approximated by the first k RCs. SSA can produce a pair of RCs with similar eigenvalues for a single periodic component of the original series.

2.2 PM analysis

SSA can be used to decompose the original time series into a series of components, such as trends, periods or quasi-periods, and noise. When these parts are sufficiently separated from each other, SSA can better reveal the roles of different signals in the initial data. The 45-year PM (PMx, PMy, polar coordinates) series covering the January 1, 1962, to December 31, 2006, period was analyzed by SSA. This PM series is taken from the EOP 08 C04 series, downloaded from the Web site of the IERS Earth Orientation Center (http://datacenter.iers.org/eop/-/somos/5Rgv/latest/214). The sampling interval in this series is one day. The EOP 08 C04 series is derived from various astro-geodetic techniques and is consistent with ITRF 2008. The accuracies of PMx and PMy in the most recent data in this series are up to 0.03 mas (Bizouard and Gambis 2011).

For the 45-year PM series, the chosen window length M was 2190 points (6 years), which is almost equal to the beat period of the annual and Chandler oscillations (Zotov 2010). The weighted correlation (w-correlations) (Hassani 2007) is used to determine the correlation coefficients between the various RCs. The weighting factor w_i is defined as

$$w_i = \begin{cases} i & 1 \le i < M^* \\ M^* & M^* \le i \le K^* \\ N - i + 1 & K^* \le i \le N, \end{cases} \tag{5}$$

where $M^* = \min(M, K)$, $K^* = \max(M, K)$, and $K = N - M + 1$. Assuming that the RC is Y_k and its corresponding elements are $y_1^k, y_2^k, \ldots, y_N^k$, the w-correlations of any two RCs can be expressed as

$$\rho_{i,j}^w = \frac{(Y^{(i)}, Y^{(j)})}{\|Y^i\|_w \|Y^j\|_w}, \quad (1 \le i, j \le N), \tag{6}$$

where $\|Y^i\|_w = \sqrt{(Y^{(i)}, Y^{(i)})}$, $\|Y^j\|_w = \sqrt{(Y^{(j)}, Y^{(j)})}$, and $(Y^{(i)}, Y^{(j)}) = \sum_{l=1}^{N} w_l y_l^i y_l^j$. Large w-correlations between RCs indicate that these components should possibly be gathered into a single group and they may correspond to the same component in the SSA decomposition.

The ith RC obtained by SSA decomposition is denoted RC i. The results of the correlation analysis of the RCs of the 45-year PM series are shown in Fig. 1. The correlation of the RCs indicated that the first 7 RCs are the independent and paired periodic components of PM. In the PMx data, RC1 and RC2, RC3 and RC4, and RC6 and RC7 are evidently three pairs of components. Using fast Fourier transform (FFT) analysis, these components were determined to be the Chandler term, the annual term, and an oscillation with a period of about 492 days, respectively. In the PMy data, RC2 and RC3, RC4 and RC5, and RC6 and RC7 represented the Chandler term, the annual term, and a period of

about 492 days, respectively. The about 492-day component may be a mathematical expression of other periodic components of PM by SSA, since the window length only takes into account the beat period of the annual and Chandler oscillations. RC5 and RC1 are the trend terms of PMx and PMy, respectively. The separated components of PMx and PMy are shown in Fig. 2.

The residual components shown in Fig. 2 which indicate that the first seven RCs are good approximations of the original series. The RMS of the remaining RCs from the PMx data is 13.0779 mas, and the RMS of the remaining RCs from the PMy data is 13.0056 mas. The amplitude of the Chandler oscillations obtained by SSA fluctuates between 150 and 200 mas, and the amplitude of the annual oscillations fluctuates between 50 and 100 mas. The trend rates in the x- and y-directions were calculated to be 1.4585 ± 0.007 mas and 3.9712 ± 0.007 mas per year, respectively. The trend rate of the PM is 4.23 mas per year. The North Pole moves to 69.85°W in the longitudinal direction with respect to the crust.

3 Prediction method

In this study, the data concerning the prediction period are regarded as the missing part, and SSA is used to predict the main components of the PM data. For the PM prediction, M and k were determined for the SSA from prior PM analysis. According to the PM analysis, the trend and main periodic terms can better approximate the original PM series by taking into account both the Chandler and annual oscillation periods when determining M. We proposed a method to extrapolate the RCs by SSA and the ARMA prediction model. The main steps (as shown in Fig. 3) are as follows.

(1) The predicted length n is set. n zero values are added to the end of the original data (of length N) to construct a PM sequence with a total length of $N + n$.
(2) Decomposition of the new series (with length $N + n$) by SSA. The n values at the end of the first RC (RC1) are selected to replace the predicted values. This process is repeated until RC1 converges. The convergent condition is such that the RMS of the difference between the two decomposed RC1 values is 0.001 mas.
(3) At the end of the first cycle, the second RC (RC2) is added to reconstruct the forecast data; the prediction data are obtained by superimposing RC1 and RC2. Step (2) is repeated until the RC1 + RC2 sequence converges.
(4) The above procedure is repeated until the prediction data are replaced with k RCs. The series of length n at the end of these RCs is the main RC prediction series of PM (denoted by k RCP).
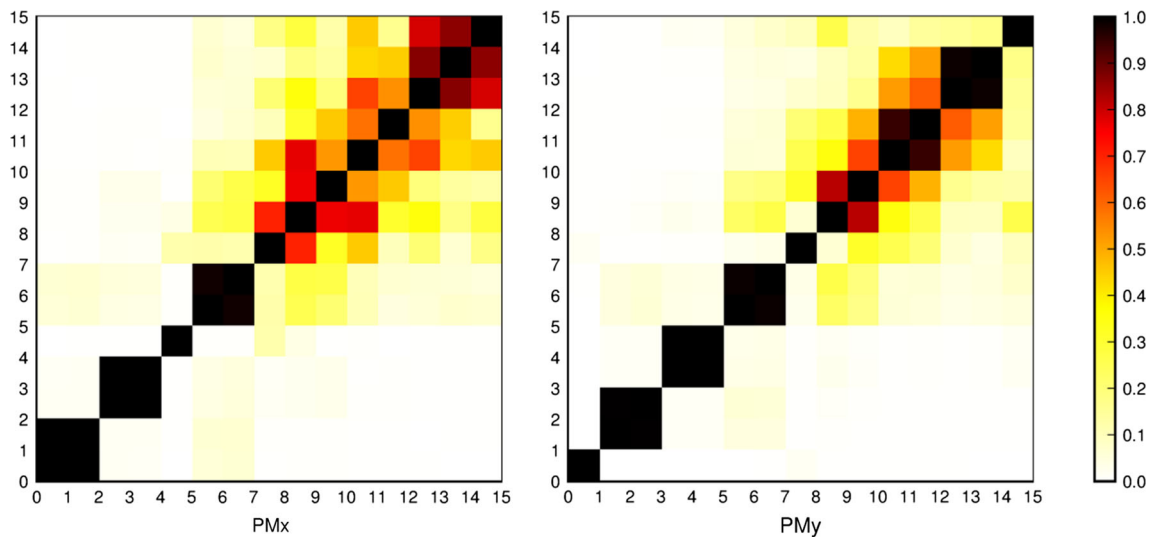
Fig. 1 Matrix of w-correlations for the first 15 RCs
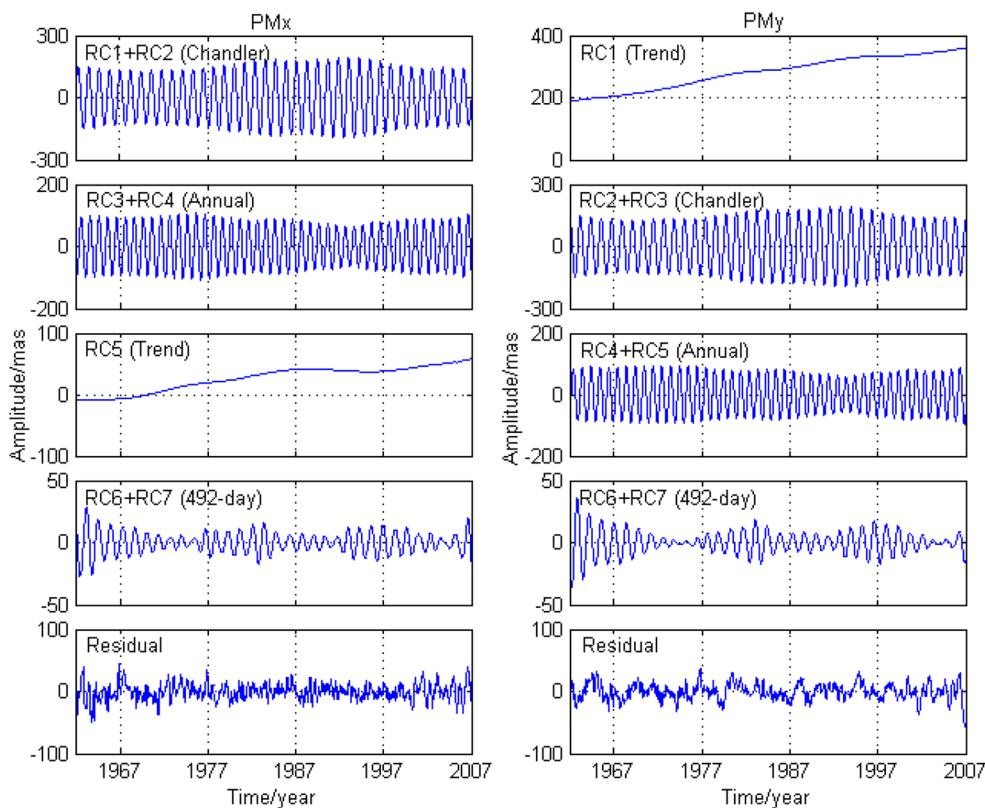
Fig. 2 Components of PMx and PMy separated by SSA

(5) The residual RC of the original PM series $\{R_N\}$ contains a number of other periodic terms and noises. Assuming that the value of R_N is related not only to its pre-p values, but also to the pre-q distracters, then according to the principles of multiple regression, the ARMA(p, q) model (Valipour et al. 2013) is

$$R_N = \beta_1 R_{N-1} + \beta_2 R_{N-2} + \cdots + \beta_p R_{N-p} - \theta_1 a_{N-1}$$
$$-\theta_2 a_{N-2} - \cdots - \theta_q a_{N-q} + a_N, \qquad (7)$$

where $\beta_i(i = 1, 2, \ldots, p)$ are the autoregressive (AR) coefficients, $\theta_i(i = 1, 2, \ldots, q)$ are the moving average (MA) coefficients, and $\{a_N\}$ is the white noise series. The extended autocorrelation function (EACF) (Cryer
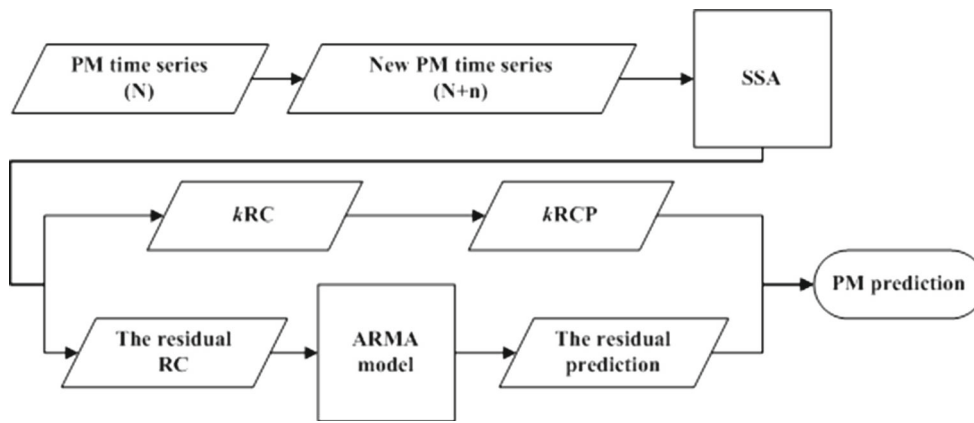
Fig. 3 Flowchart of the SSA + ARMA method for PM prediction

and Chan 2008) is used to determine the orders of p and q. The parameters of the model are chosen by the maximum likelihood estimate method. The predictions of the residual series are performed according to the determined ARMA(p, q) model.

(6) Combining the SSA prediction results with the prediction ARMA results gives the final predictions.

4 Prediction of the polar motion

In this study, EOP 08 C04 PM data from 1962 to 2016 were selected for the validation of SSA + ARMA predictions. The PM from January 1, 2009, to the predicted start time was used as the original PM series. The principle components of two-year lead time PMs (denoted by 7RCP) were predicted using the proposed SSA prediction method (the first seven RCs and the window length $M = 2190$). The start times of the two-year lead time PMs were January 2, 2007, January 1, 2008, January 6, 2009, January 5, 2010, January 4, 2011, January 3, 2012, January 1, 2013, and December 31, 2013. Decomposition of the original PM series concerning the prediction period was performed by SSA to obtain the first seven RCs (denoted by 7RC). The original, 7RC, and 7RCP series for each prediction period are shown in Fig. 4.

Figure 4 shows that the first seven RCs obtained by SSA agree well with the first seven RCs of the original PM series over multiple prediction periods. From Sect. 2.2, it can be seen that the reconstructed series of the first seven RCs can accurately represent the original series. Therefore, the principal components of a PM series can be predicted effectively by SSA. The correlations between the predicted RCs and the RCs of the original PM series were analyzed. The results are shown in Table 1. The highest correlation coefficients were determined to be between the 5RCP series and the 5RC series of the original PM series. The corre-

lation between the 7RCP series and the 7RC series of the original PM series is relatively poor. However, the correlation between the 5RCP series and the original PM series is weaker than that of the 7RCP series, which indicates that increasing the number of predicted RCs will also increase the uncertainty of the principal component predictions. The trend, annual, and Chandler terms were relatively stable, with about 492-day periodic term, which indicates that SSA is capable of reliably reconstructing the stable principal components.

The above prediction results show that SSA can effectively predict the medium- and long-term principal components of PM. However, there was a random fluctuation in the remaining SSA components from Sect. 2.2, which caused a ±50 mas deviation from the starting point of the short-term predictions, as shown in Fig. 4. Therefore, the ARMA(p, q) model can be used to extrapolate the residual series. The EACF indicated that the ARMA (2,8) model was suitable for the residual SSA series. The extrapolation results of the ARMA model were combined with the main component predictions of the SSA over the whole 2-year PM predictions. To evaluate the precision of the PM prediction series, the predictions were compared with the corresponding IERS EOP 08 C04 PM series. The prediction accuracies are measured by RMSE as well. The error bars of RMSE were computed by $\hat{\sigma}(\text{RMSE})_i = \frac{\text{RMSE}_i}{\sqrt{2n_p}}$, where i is the prediction length and n_p is the number of predictions (Kalarus et al. 2010).

IERS Bulletin A contains predicted PMs for the following year, which are updated every seven days by the IERS (Stamatakos et al. 2011). To verify the reliability of the SSA + ARMA method, the accuracy of the predicted series was compared with the accuracy of the IERS Bulletin A predictions (http://datacenter.iers.org/eop/-/somos/5Rgv/getTX/6). The systematic prediction errors of the two methods are shown in Fig. 5. The RMSEs of the sixteen forecast periods are shown in Fig.6.

Fig. 4 730-day PM series (gray line), 7RC reconstructed series (red dotted line), and 7RCP prediction series (black line) from 2007.1 to 2014.7
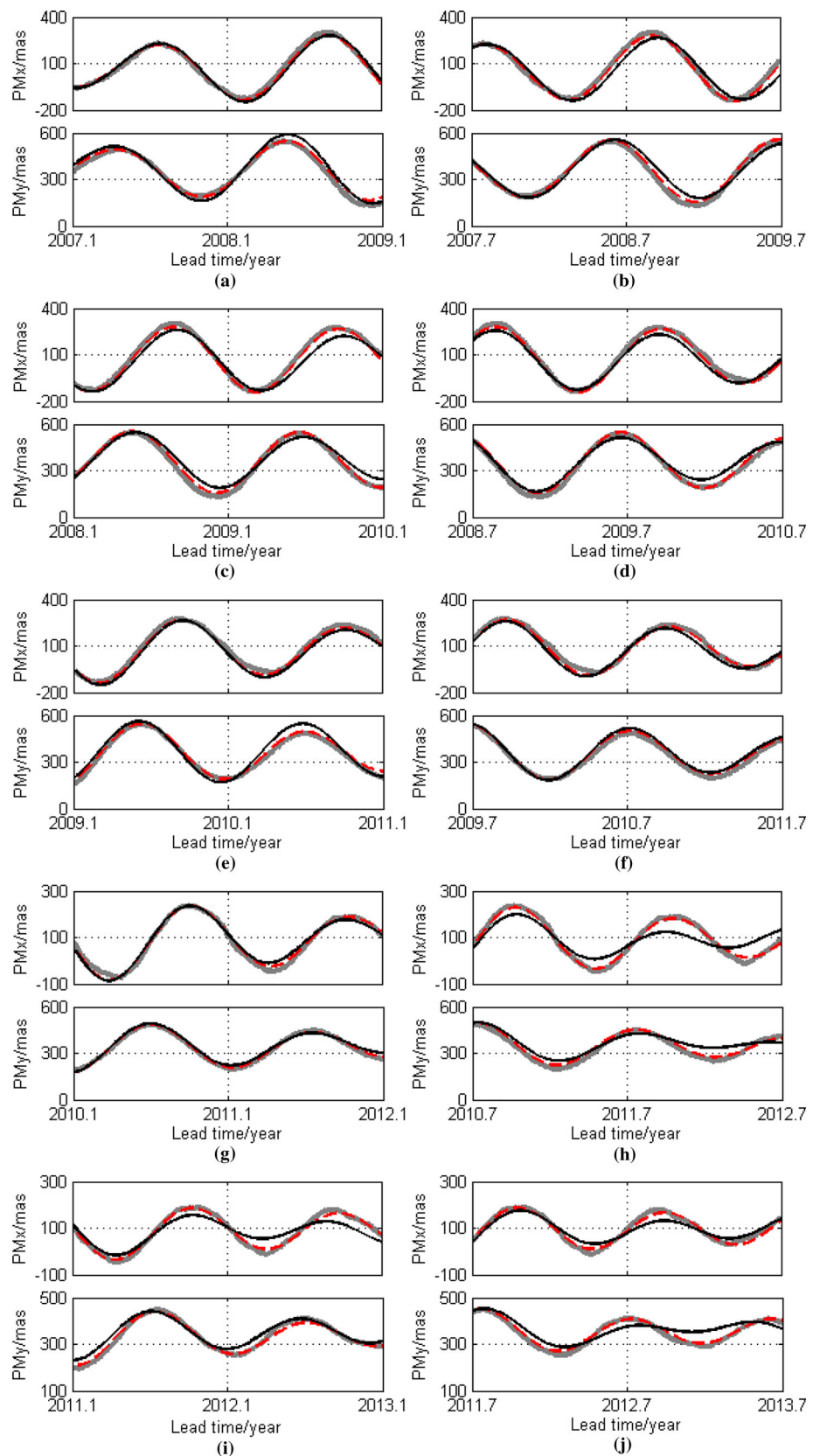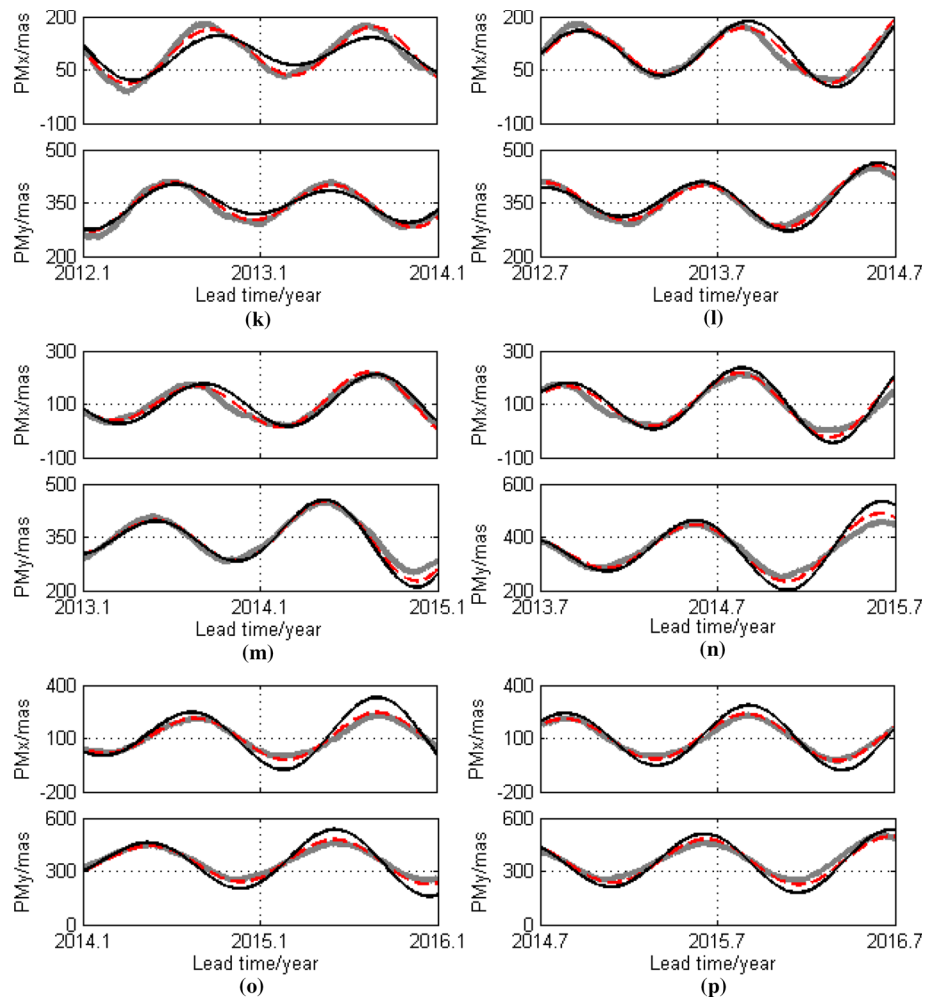
Fig. 4 continued

Table 1 Correlation coefficients of the predicted RCs with the RCs of the original PM series

Prediction time	5RCP–5RC		7RCP–7RC		5RCP-PM series		7RCP-PM series	
	X	Y	X	Y	X	Y	X	Y
2007.1–2009.1	0.999	0.9994	0.9964	0.9974	0.9859	0.9846	0.9885	0.9856
2007.7–2009.7	0.9963	0.9954	0.9779	0.9811	0.9933	0.9942	0.9638	0.9676
2008.1–2010.1	0.9963	0.9965	0.986	0.9854	0.995	0.997	0.9839	0.9816
2008.7–2010.7	0.9961	0.9993	0.9963	0.9927	0.9959	0.996	0.9939	0.9903
2009.1–2011.1	0.9996	0.9947	0.999	0.9846	0.9935	0.9857	0.9967	0.9788
2009.7–2011.7	0.9971	0.9995	0.9903	0.9991	0.9873	0.9753	0.9829	0.9908
2010.1–2012.1	0.9992	0.9996	0.9991	0.998	0.9609	0.9482	0.9856	0.9896
2010.7–2012.7	0.9598	0.9801	0.9051	0.9565	0.8669	0.8832	0.9028	0.942
2011.1–2013.1	0.9564	0.9813	0.9315	0.973	0.8555	0.9383	0.9311	0.9764
2011.7–2013.7	0.9706	0.9488	0.9585	0.8663	0.8761	0.8773	0.9536	0.8508
2012.1–2014.1	0.9919	0.9966	0.9553	0.9785	0.9077	0.9008	0.9368	0.9687
2012.7–2014.7	0.9877	0.996	0.9263	0.9453	0.9262	0.965	0.8707	0.9205
2013.1–2015.1	0.9888	0.9994	0.9556	0.9978	0.9422	0.9736	0.9334	0.9777
2013.7–2015.7	0.9987	0.9994	0.9943	0.9983	0.9697	0.9827	0.9757	0.9789
2014.1–2016.1	0.9945	0.9976	0.9908	0.9955	0.9916	0.9915	0.9742	0.9841
2014.7–2016.7	0.9961	0.9968	0.9915	0.9904	0.9884	0.98	0.9791	0.9756
MEAN	0.9892	0.9925	0.9721	0.9774	0.9522	0.9608	0.9595	0.9662

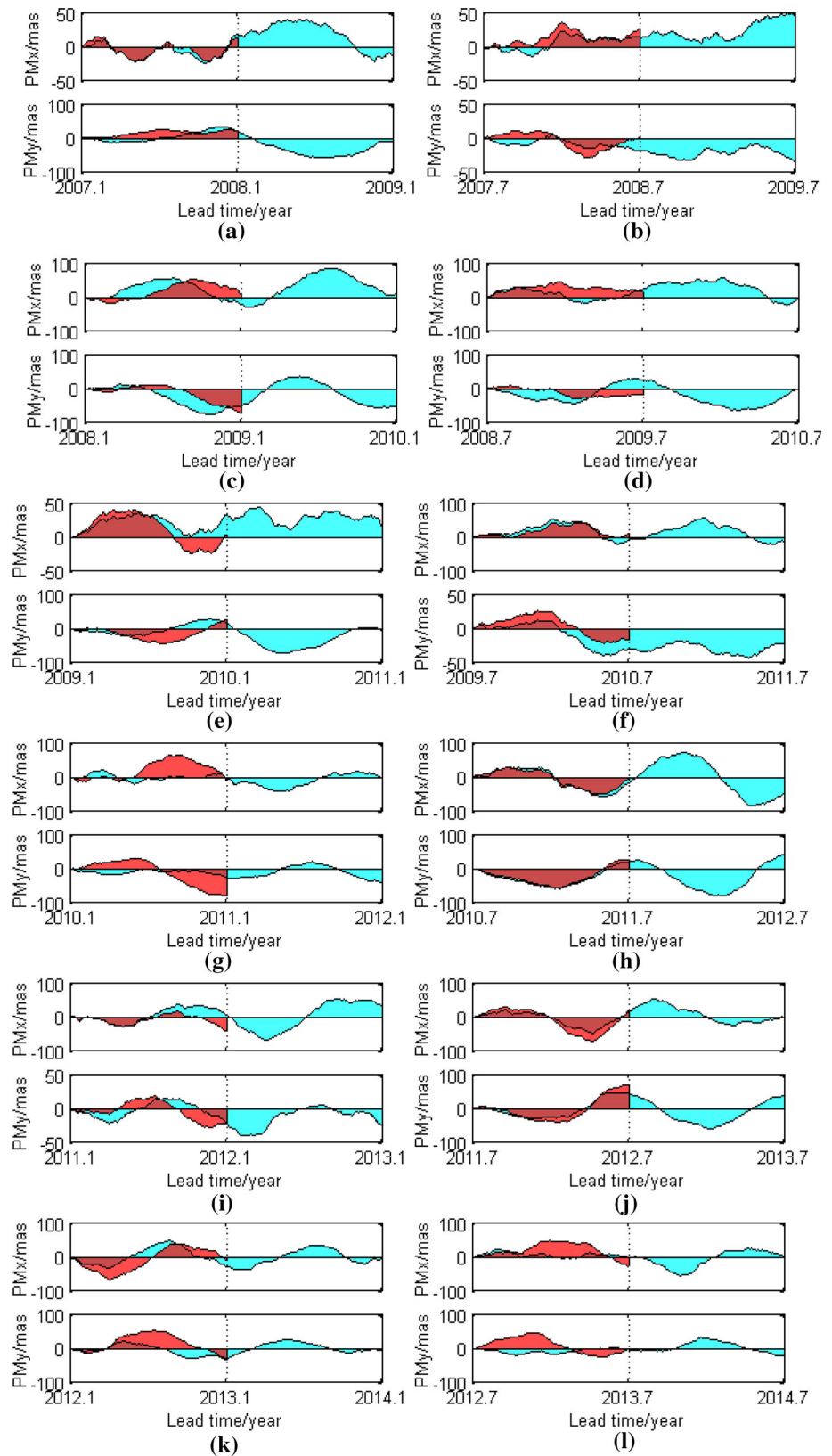**Fig. 5** Systematic prediction errors of the IERS Bulletin A and SSA + ARMA predictions

Fig. 5 continued

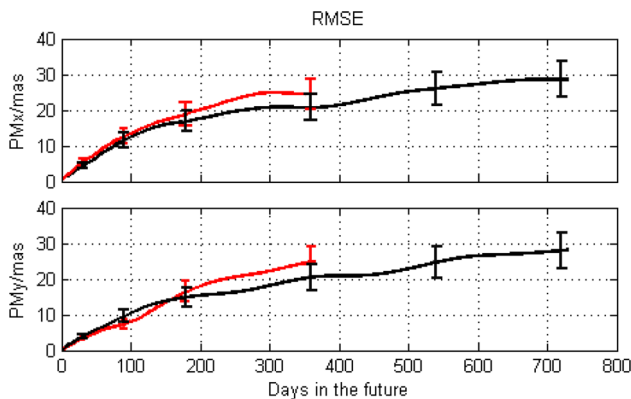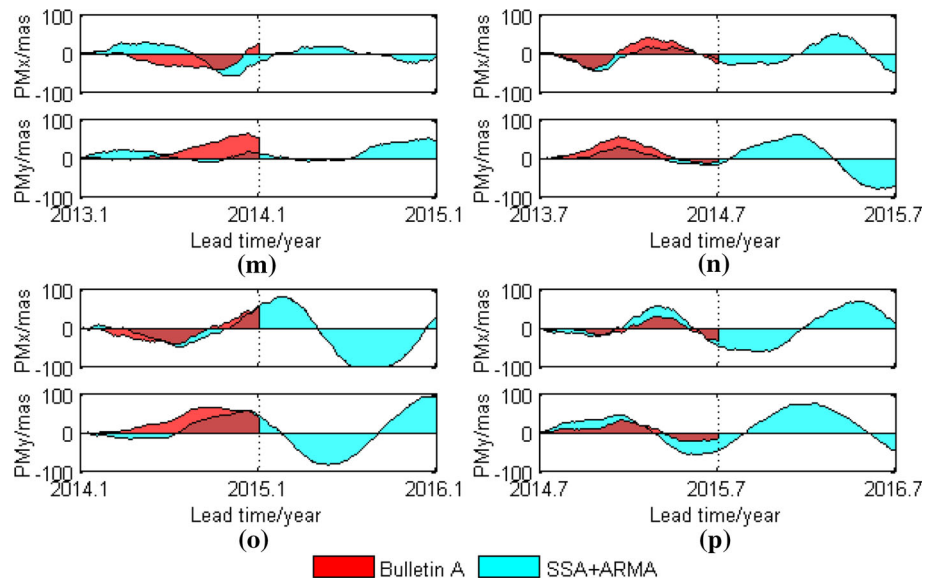**(m)** **(n)** **(o)** **(p)**

Bulletin A SSA+ARMA

**Fig. 6** RMSE of the IERS Bulletin A (red) and SSA + ARMA predictions (black)

Figure 5 shows that the systematic prediction errors in the SSA + ARMA predictions were reasonably low in the 730-day forecast, and lower still in the 365-day forecast. Figure 6 indicates that the RMSE of SSA + ARMA is slightly lower than that of the Bulletin A predictions for PMx over one year, and significantly lower from the 157th day prediction length

for PMy. The RMSEs are shown in Table 2. For PMx and PMy, the RMSEs of SSA + ARMA in the 180-day predictions are 16.84 and 14.86 mas, respectively, which are lower than those of 18.95 and 16.44 mas for the Bulletin A predictions. The RMSEs for PMx and PMy from SSA + ARMA in the 360-day predictions were 20.67 and 20.42 mas, respectively, lower than those of 24.46 and 24.78 mas for Bulletin A. The RMSEs of the overall PMx and PMy SSA + ARMA predictions were 28.61 and 27.95 mas, respectively.

The RMSE of SSA + ARMA increased slowly with the increase in the forecasting time, and the prediction accuracy of 720 and 540 days just showed several mas more than that of 360 days. The distribution of the absolute errors of PM prediction (see Fig. 7) shows that the proportions of the absolute errors less than 30 mas of PMx and PMy in the whole 720 days are 70 and 70%, respectively. In the 360–720 days, the proportions are 59 and 60%, respectively. The forecasting errors in the 360–720 days are limited to a small range. The SSA is capable of reliably reconstructing the stable principal components. It enables the SSA + ARMA particularly suitable for long-term prediction.

Table 2 Comparison of the RMSE (mas) of the Bulletin A and SSA + ARMA predictions

Lead day	Bulletin A				SSA + ARMA			
	PMx	$\hat{\sigma}_{PMx}$	PMy	$\hat{\sigma}_{PMy}$	PMx	$\hat{\sigma}_{PMx}$	PMy	$\hat{\sigma}_{PMy}$
30	5.51	0.97	3.29	0.58	4.26	0.75	3.87	0.68
90	12.63	2.23	7.34	1.29	11.56	2.04	9.61	1.70
180	18.95	3.35	16.44	2.91	16.84	2.98	14.86	2.63
360	24.46	4.32	24.78	4.38	20.67	3.65	20.42	3.61
540	–	–	–	–	26.05	4.61	24.66	4.36
720	–	–	–	–	28.61	5.06	27.95	4.94
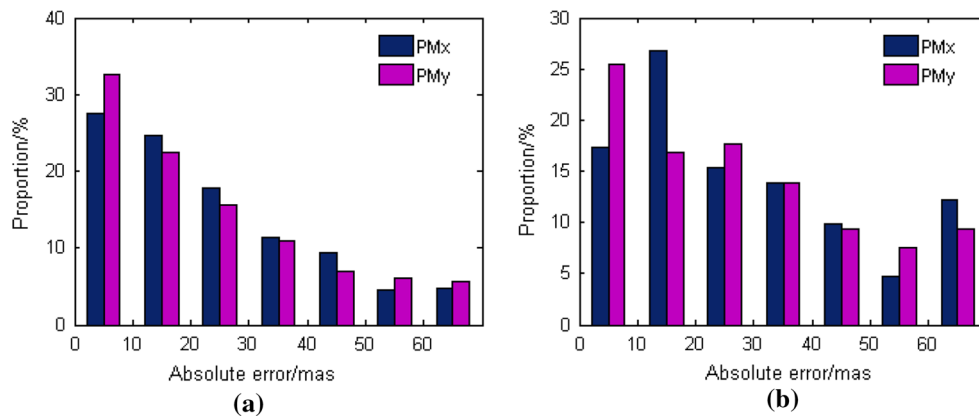
Fig. 7 Distribution of the absolute errors in the whole 720 days (a) and the 360–720 days (b)

During the whole period, the prediction accuracy of PMy is better than that of PMx, as the correlation coefficient between 7RCP for PMy and the original series is greater than that for the PMx. Overall, the results show that the proposed SSA + ARMA method can effectively predict PM.

5 Conclusions

In this study, the 45-year PM series data from January 1, 1962, to December 31, 2006, were analyzed by SSA. The results show that SSA can effectively separate and reconstruct the trend, annual, Chandler, and 492-day periodic terms of PM. The first seven RCs were suitable approximations of the original series. We described a method of predicting the main components of PM using SSA, derived from the basic SSA principles and algorithm. Multiple two-year PM predictions showed that the average correlation coefficients between the principal component prediction series and the principal component series of PMx and PMy were 0.9721 and 0.9774, respectively. The average correlation coefficients between the principal component prediction series and the PM series were 0.9595 and 0.9662, respectively, which indicated that SSA could effectively predict long-term PM.

To reduce the influence of the remaining components of the SSA on the PM predictions, an ARMA model was constructed using the residual components, to improve the accuracy of the short-term PM predictions. The RMSEs of SSA + ARMA in the short- and long-term predictions were low. Compared with predictions published in IERS Bulletin A, the RMSE of SSA + ARMA was smaller over 180- and 360-day lead times. The RMSE of SSA + ARMA increases slowly with increasing forecast time, and the 720-day PM prediction showed good precision. Overall, these results indicate that the proposed SSA + ARMA method has good reliability and high precision for the prediction of PM.

References

Akulenko LD, Kumakshev SA, Markov YG, Rykhlova LV (2002) Forecasting the polar motions of the deformable Earth. Astron Rep 46(10):858–866. doi:10.1134/1.1515097

Akyilmaz O, Kutterer H (2004) Prediction of Earth rotation parameters by fuzzy inference systems. J Geod 78(1):82–93. doi:10.1007/s00190-004-0374-5

Akyilmaz O, Kutterer H, Shum CK, Ayan T (2011) Fuzzy-wavelet based prediction of Earth rotation parameters. Appl Soft Comput 11(1):837–841. doi:10.1016/j.asoc.2010.01.003

Beckers JM, Rixen M (2003) EOF calculations and data filling from incomplete oceanographic datasets. J Atmos Ocean Tech 20(12):1839–1856. doi:10.1175/1520-0426(2003)020<1839:ECADFF>2.0.CO;2

Bizouard C, Gambis D, (2009) The combined solution C04 for Earth orientation parameters consistent with international terrestrial reference frame, 2005. Geodetic reference frames, pp 265–270. Springer, Berlin. doi:10.1007/978-3-642-00860-3_41

Bizouard C, Gambis D (2011) The combined solution C04 for Earth orientation parameters consistent with international terrestrial reference frame 2008. IERS Earth orientation. IERS notice 2011. ftp://hpiers.obspm.fr/iers/eop/eopc04/C04.guide.pdf

Broomhead DS, King GP (1986) Extracting qualitative dynamics from experimental data. Physica D 20:217–236. doi:10.1016/0167-2789(86)90031-X

Chen JL, Wilson CR (2005) Hydrological excitations of polar motion 1993–2002. Geophys J Int 160(3):833–839. doi:10.1111/j.1365-246X.2005.02522.x

Chen Q, Dam VT, Sneeuw N, Collilieux X, Weigelt M, Rebischung P (2013) Singular spectrum analysis for modeling seasonal signals from GPS time series. J Geodyn 72:25–35. doi:10.1016/j.jog.2013.05.005

Choi KK, Ray J, Griffiths J, Bae TS (2013) Evaluation of GPS orbit prediction strategies for the IGS ultra-rapid products. GPS Solut 17(3):403–412. doi:10.1007/s10291-012-0288-2

Cryer JD, Chan KS (2008) Time series analysis: with application in R. Springer, Berlin, pp 249–276. doi:10.1007/978-0-387-75959-3_11

Guo JY, Han YB (2009) Seasonal and inter-annual variations of length of day and polar motion observed by SLR in 1993–2006. Chin Sci Bull 54(1):46–52. doi:10.1007/s11434-008-0504-1

Hassani H (2007) Singular spectrum analysis: methodology and comparison. J Data Sci 5(2):239–257

Jin SG, Hassan AA, Feng GP (2012) Assessment of terrestrial water contributions to polar motion from GRACE and hydrological models. J Geodyn 62:40–48. doi:10.1016/j.jog.2012.01.009

Kalarus M, Schuh H, Kosek W, Akyilmaz O, Bizouard Ch, Gambis D, Gross R, Jovanovic B, Kumakshev S, Kutterer H, Ma L, Mendes Cerveira PJ, Pasynok S, Zotov L (2010) Achievements of the Earth orientation parameters prediction comparison campaign. J Geod 84(10):587–596. doi:10.1007/s00190-010-0387-1

Kondrashov D, Ghil M (2006) Spatio-temporal filling of missing points in geophysical data sets. Nonlinear Process Geophys 13(2):151–159

Kondrashov D, Berloff P (2015) Stochastic modeling of decadal variability in ocean gyres. Geophys Res Lett 42(5):1543–1553. doi:10.1002/2014GL062871

Kondrashov D, Shprits Y, Ghil M (2010) Gap filling of solar wind data by singular spectrum analysis. Geophys Res Lett 37(15):L15101. doi:10.1029/2010GL044138

Kosek W, McCarthy DD, Luzum BJ (1998) Possible improvement of Earth orientation forecast using autocovariance prediction procedures. J Geod 72(4):189–199. doi:10.1007/s001900050160

Kosek W, Kalarus M, Niedzielski T (2007) Forecasting of the Earth orientation parameters comparison of different algorithms. In: Capitaine N (ed) Proceedings of the "Journèes systèmes de deréférence spatio-temporels (2007) Observatoire de Paris, 17–19 Sept 2007, Paris, France. pp 155–158

Liao D, Wang Q, Zhou Y, Liao XH, Huang CL (2012) Long-term prediction of the Earth orientation parameters by the artificial neural network technique. J Geodyn 62:87–92. doi:10.1016/j.jog.2011.12.004

Rial JA, Oh J, Reischmann E (2013) Synchronization of the climate system to eccentricity forcing and the 100,000-year problem. Nat Geosci 6:289–293. doi:10.1038/ngeo1756

Schoellhamer DH (2001) Singular spectrum analysis for time series with missing data. Geophys Res Let 28(16):3187–3190. doi:10.1029/2000GL012698

Schuh H, Behrend D (2012) VLBI: a fascinating technique for geodesy and astrometry. J Geodyn 61:68–80. doi:10.1016/j.jog.2012.07.007

Schuh H, Nagel S, Seitz T (2001) Linear drift and periodic variations observed in long time series of polar motion. J Geod 74(10):701–710. doi:10.1007/s001900000133

Schuh H, Ulrich M, Egger D, Müller J, Schwegmann W (2002) Prediction of Earth orientation parameters by artificial neural networks. J Geod 76(5):247–258. doi:10.1007/s00190-001-0242-5

Shen Y, Guo JY, Zhao C, Yu X, Li J (2015) Earth rotation parameter and variation during 2005–2010 solved with LAGEOS SLR data. Geod Geodyn 6(1):55–60. doi:10.1016/j.geog.2014.12.002

Stamatakos N, Luzum B, Stetzler B, Shumate N, Carter MS (2011) Recent improvements in IERS rapid service/prediction center products. In: Proceedings of the Journées Systèmes de référence spatio-temporels, pp 184–187

Su X, Liu L, Hsu H, Wang G (2014) Long-term polar motion prediction using normal time–frequency transform. J Geod 88(2):145–155. doi:10.1007/s00190-013-0675-7

Valipour M, Banihabib ME, Behbahani SMR (2013) Comparison of the ARMA, ARIMA, and the autoregressive artificial neural network models in forecasting the monthly inflow of Dez dam reservoir. J Hydrol 476:433–441. doi:10.1016/j.jhydrol.2012.11.017

Vautard R, Ghil M (1989) Singular spectrum analysis in nonlinear dynamics, with applications to paleoclimatic time series. Physica D 35(3):395–424. doi:10.1016/0167-2789(89)90077-8

Wang X, Cheng Y, Wu S, Zhang K (2016) An enhanced singular spectrum analysis method for constructing nonsecular model of GPS site movement. J Geophys Res 121(3):2193–2211. doi:10.1002/2015JB012573

Wyatt MG, Kravtsov S, Tsonis AA (2012) Atlantic multi decadal oscillation and northern hemisphere's climate variability. Clim Dyn 38(5):929–949. doi:10.1007/s00382-011-1071-8

Xu X, Zhou Y (2015) EOP prediction using least square fitting and autoregressive filter over optimized data intervals. Adv Space Res 56(10):2248–2253. doi:10.1016/j.asr.2015.08.007

Xu X, Zhou Y, Liao X (2012) Short-term earth orientation parameters predictions by combination of the least-squares, AR model and Kalman filter. J Geodyn 62:83–86. doi:10.1016/j.jog.2011.12.001

Yao YB, Yue S, Chen P (2013) A new LS + AR model with additional error correction for polar motion forecast. Sci China Earth Sci 56(5):818–828. doi:10.1007/s11430-012-4572-3

Zotov L (2010) Dynamical modeling and excitation reconstruction as fundamental of Earth rotation prediction. Artif Satell 45(2):95–105. doi:10.2478/v10018-010-0010-y